IV International Conference on Particle-based Methods – Fundamentals and Applications
PARTICLES 2015
E. Oñate, M. Bischoff, D.R.J. Owen, P. Wriggers & T. Zohdi (Eds)

A PORE-SCALE APPROACH OF TWO-PHASE FLOW IN GRANULAR POROUS MEDIA

C. YUAN[1], B. CHAREYRE[2] AND F. DARVE[3]

[1] Grenoble-INP, UJF, CNRS UMR 5521, 3SR Lab.
BP 53, 38041, Grenoble cedex 9, France
chao.yuan@3sr-grenoble.fr

[2] Grenoble-INP, UJF, CNRS UMR 5521, 3SR Lab.
BP 53, 38041, Grenoble cedex 9, France
bruno.chareyre@3sr-grenoble.fr

[3] Grenoble-INP, UJF, CNRS UMR 5521, 3SR Lab.
BP 53, 38041, Grenoble cedex 9, France
felix.darve@3sr-grenoble.fr

Key words: Pore-scale Modeling, Network Models, Two-phase Flow, DEM, Drainage

Abstract. A pore-scale model is presented for simulating two-phase flow in granular materials. The solid phase is idealized as dense random packings of polydisperse spheres, generated with the discrete element method (DEM). The pore space is conceptualized as a network of pores connected by throats, which is obtained by using regular triangulation. Theoretical formulas for calculating geometrical properties and entry capillary pressure for given pores are developed by extending the Mayer and Stowe-Princen (MS-P) theory of drainage. Such relationships are employed in the network for defining as local invasion criteria, so that the drainage can be represented by the replacement of W-phase when the threshold value is reached. The events of W-phase entrapment are considered during the coupling procedures. This pore-scale model is verified by comparing simulation results with experimental data of quasi-static drainage experiments in a synthetic porous medium. The simulated $P^c - S^w$ curve in primary drainage is in agreement with the experimental one.

1 INTRODUCTION

Understanding transport properties of multiphase flow in porous media is of great importance for many areas of engineering and science, such as oil recovery, agriculture irrigation and environmental restoration. Although most of these problems describe such flow process at the macro-scale, pore-scale modeling provides an important means to improve our understanding of the insight physical processes. In order to simulate large

domains, one often represent the porous medium by a pore-network, in which the void space of the medium is represented by a lattice of wide pores connected by narrow throats. By using appropriate physical laws that govern the transport and arrangement of fluids in system, network can then be made to replicate experimental measurements at the microscopic scale. The use of network modeling was pioneered by Fatt in the 1950s[9], who derived capillary pressure curves of primary drainage and computed pore size distributions in a network of interconnected pores. Since then, numerous researchers have contributed to our present understanding of multiphase flow in pore-scale with network[16, 19, 2, 14, 17, 11].

The method considered in this study is similarly devoted to the pore-scale modeling of the transport process of multiphase flow, but important differences are also noticeable in the geometrical idealization of the pore space and network modeling. These difference are mainly due to the spherical geometry of the solid particles and to the pore space decomposition technique. This study represents a first step in the direction of developing a fully coupled, computationally efficient model combining two-phase flow and deformation in porous media. In particular, we will focus our effort on the faithful approximation of the capillary pressures applied by the fluid-fluid interface on solid grains and of the arrangements of phases displacements, with the aim of incorporate these pressures and arrangements in the discrete element method (DEM) computation[7].

2 PORE-SCALE NETWORK

We propose a pore-scale network model for simulating two-phase flow in granular materials. The solid phase is idealized as dense random packings of polydisperse spheres, generated with the discrete element method (DEM)[22]. The decomposition of the pore space is obtained in three dimensions by a using Regular Triangulation method, in which the void of porous media is conceptualized as a network of pores connected by throats. A similar network was introduced recently for the so called the Pore-scale Finite Volume scheme (PFV) for one-phase flow. It is able to reflect in a natural way the deformation of the porous material system. Here it will be discussed briefly; a more detailed description can be found in [5] and [3].

Regular Triangulation (or referred as weighted Delaunay triangulation) generalizes classical Delaunay triangulation to weighted points, where weights account for the size of the spheres[8]. The dual Voronoi graph of regular triangulation is entirely contained in voids between solid spheres. Such network scheme can ideally be assigned to solve the flow path problem within the porous sample. A typical network of Regular Triangulation is shown in Fig.1. Based on this decomposition, a "pore" in 3D is bounded by four solid spheres with respective radius $R\{r_1, r_2, r_3, r_4\}$, which are arranged forming a simple tetrahedron packing order. Pore body volume is defined to be the irregular cavity within the tetrahedron(see Fig.2a). The shape of pore throat is considered to be the cross section extending within tetrahedral facets, thus the volume of throat is assumed to be 0. Specifically, the geometry of entry pore throat is a critical cross-sectional area quantified by the multiphase

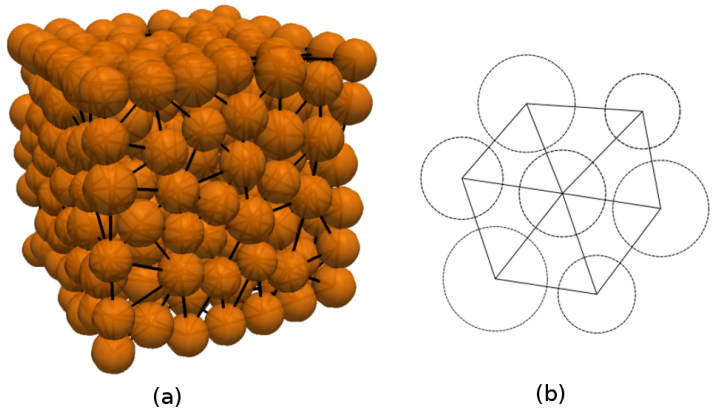

Figure 1: Definition of pore network for packing of spheres, generated by regular triangulation in 3D(a) and 2D(b).

contact lines(shown in Fig.2b).

Since each pore is a tetrahedron, it has four neighbors, resulting in a lattice of connectivity four. Although the similar network can be found in other models [15, 10], those decomposition techniques are limited by solid particle size, in which the triangulation can only be assigned in packing of equal spheres. In this model, the network definition applies polydisperse sphere packings. The only restriction on this geometrical description is that the center of one sphere should not lie inside another sphere. As such, contact or even moderate overlaps between adjacent spheres are allowed.

3 DRAINAGE MODEL

3.1 Local rules

The phenomena of multiphase flow in porous media can be divided into quasi-static regime and dynamic ones. For two-phase flow, or referred as drainage and imbibition, in the absence of gravity, the conventional immiscible displacement can be described by two dimensionless numbers, the viscosity ratio M and the capillary number C_a,

$$M = \frac{\mu_{inv}}{\mu}, C_a = \frac{\mu v}{\sigma} \tag{1}$$

where μ_{inv} is the viscosity of invading phase, μ is the viscosity of receding phase, v is the receding phase average or macroscopic velocity and σ is the interfacial tension between two fluid phases([13, 12]). The limit of "quasi-static" flow is defined by C_a closed to 0.

The model we propose is aiming to simulate the primary drainage phenomenon of air-water system, or typically, more generally nonwetting-wetting (NW-W) systems. We hypothesize the drainage process is in a quasi-static regime, in which dynamic effects is in absent and the flow is dominated by capillary forces. Thus, we can neglect the effects of phases viscosity during the process. The porous within a fluid phase is uniform in every connected domain.

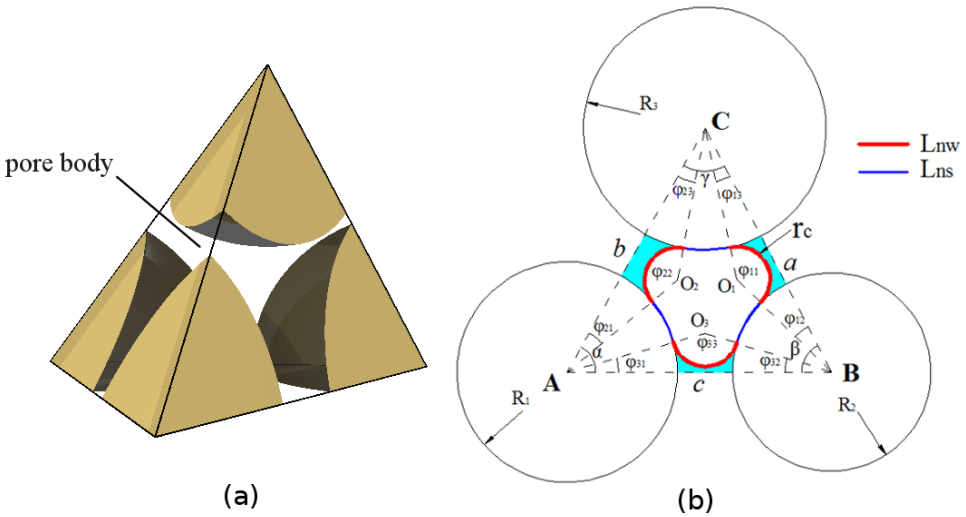

Figure 2: Pore geometry. (a)A pore defined by tetrahedral element of the finite volume decomposition. (b)Definition of pore throat geometry. r_c is the curvature of meniscus; L_{nw} is the length of contact line between nonwetting and wetting phases; L_{ns} is the length of contact line between nonwetting and solid phases.

The drainage process is controlled by the capillary pressure P^c, i.e., the pressure difference between NW-phase and W-phase. The invasion of one pore is controlled by the associated pore throats. Because the entry capillary pressure of pore body is smaller than that of pore throat, after the invasion of throat, the body is filled by NW-phase spontaneously. In principle, the receding W-phase can be present in the involved domain in the form of disconnected pendular rings left behind. The relationship between the capillary pressure and volume of liquid bridge can be found in our previous research[20, 21]. However, in this model, we assume this volume is negligible. So there is no saturation associated with corner W-phase. Thus the state of a local pore unit is in binary condition, i.e., the pore is either filled with W-phase or with NW-phase.

A relationship between capillary pressure P^c, interfacial tension, σ, and curvature of the NW-W interface, C, is given by the Young-Laplace equation,

$$P^c = \sigma C \tag{2}$$

The curvature C is fixed by the boundary conditions of NW-phase, W-phase and solid particle surface. However, in a complex pore geometry, the curvature is difficult to define. So a more clearly knowledge of connection among P^c, C and pore geometry is required.

3.2 Determination of entry capillary pressure

The drainage process is assumed in quasi-static regime, so P^c is applied into porous media to result in from one equilibrium state to another. The NW-phase invasion is locally controlled by entry capillary pressure P_e^c of pore throat. The determination of P_e^c

is based on MS-P (Mayer-Stowe-Princen) method, which follows the balance of forces for NW-W interface of pore throat [16, 18].

$$\sum F = F^p + T^\sigma = 0 \tag{3}$$

where, F^p is the capillary force acting on pore throat section domain; T^σ is the total tension force along multi-phase contact lines. The same strategy for solving P_e^c can also be found in [14] and [11]. For completeness, we recall the generic aspect of the MS-P method hereafter.

As described in the previous section, the geometry of pore throat has a mixed cross-sectional shape extending in the facet of tetrahedral pore. Fig.2b shows the schematic cross section of a local pore throat formed by solid phase surface and NW-W interface. In local drainage of pore unit, when NW-phase invades pore body, W-phase will remain in the corners of throats along the fictious tube. The longitudinal curvature of the resulting interface inside the tube is zero[11]. The critical curvature of three menisci extending within throat section, i.e., the curvature of contact lines between NW-phase and W-phase, are equal. Let that radius be denoted by entry capillary radius r_c. Then, following Young-Laplace equation, P_e^c can be written:

$$P_e^c = P^n - P^w = \frac{\sigma^{nw}}{r_c} \tag{4}$$

in which, P^n and P^w are pressure of NW-phase and W-phase; σ^{nw} is NW-W interface tension.

According to the geometry of pore throat we defined in Fig.2b, the forces acting on interface can be written:

$$F^p = P_e^c A_n \tag{5}$$

$$T^\sigma = L_{nw}\sigma^{nw} + L_{ns}\sigma^{ns} - L_{ns}\sigma^{ws} \tag{6}$$

where, A_n is the area of pore throat section; L_{nw} and L_{ns} are total length of NW-W contact lines and NW-Solid contact lines, respectively. The multiphase interfacial tensions, σ^{ns}, σ^{ws} and σ^{nw} have a relationship with contact angle θ, defined by Young's equation,

$$\sigma^{ns} - \sigma^{ws} = \sigma^{nw}\cos\theta \tag{7}$$

Then Eq.6 will be read,

$$T^\sigma = (L_{nw} + L_{ns}\cos\theta)\sigma^{nw} \tag{8}$$

In a local pore geometry, Eq.5 and Eq.8 can be expressed by the functions of r_c (see Appendix), so the equilibrium state in Eq.3 can be implicitly described by r_c:

$$\sum F(r_c) = F^p(r_c) + T^\sigma(r_c) = 0 \tag{9}$$

Function of $\sum F(r_c)$ is monotonic; the value boundary of r_c can be obtained by following the geometry of pore throat. Therefore, r_c can be solved by numerical technique. Finally, P_e^c can be determined by Eq.4.

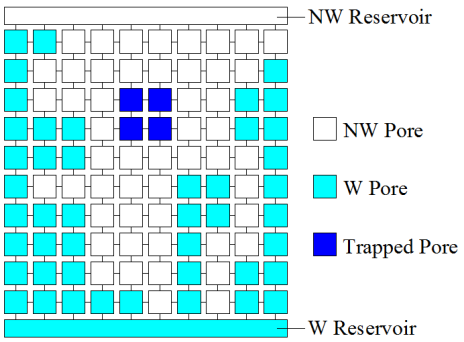

Figure 3: Demonstration of NW-phase invasion and W-phase trapping in network (in 2D mapping for clarify).

3.3 Drainage and entrapment of W-phase

Each tetrahedral pore has four neighboring pores, thus the coordination number in 3-D is four. In order to explain the invasion logic of our model, herein we project the system of 3-D network to a 2-D lattice mapping (see Fig.3). Pore bodies and throats are represented by squares and line bondings respectively. Different flags are assigned to the pores for tracking the flow path, which can dynamically record the pore states and the connectivity of different regions with the reservoirs. A search algorithm is employed for updating those states during invasion.

Initially, the porous media is saturated, and the top and bottom boundaries are connected to NW and W reservoirs, respectively. Drainage starts by increasing the capillary pressure P^c, in which we increase the local pressure of NW reservoir P^n and keep local pressure of W reservoir P^w constant. A search is executed on the pore throats which are connecting with NW reservoir, to locate the easiest entrance for invasion. The first displacement of an interface, also referred to as Haines jump, happens when local P^c surpasses the minimum threshold, e.g. the local entry capillary pressure $P_e^c(i)$ of pore unit i. After pore i being drained, a recursion algorithm check whether the interface may progress further to next adjacent pores. Such NW-phase percolation will be performed until no more pores can be drained. Then a new equilibrium is achieved, and the state flags are updated for next step of drainage. So the Haines jump events maybe not only displace the W-phase pore-by-pore, but could also involve pore clusters. Such discontinuous changes of the W-phase content can also be verified by experimental tests[6]. As the NW-phase is invading, the W-phase may form clusters of pores which are disconnected from the W reservoir. It is assumed that disconnected regions remain saturated by a fixed amount of the W-phase throughout subsequence increase of P^c. In order to identify this entrapment events, a dynamic search rule is employed during each step of drainage by assigning a Trapped Pore flag(as seen in Fig.3).

3.4 Implementation

The network has been implemented in C++[5]. The C++ library CGAL [1] is used for the regular triangulation procedure. Geometry for determination of entry capillary pressure and local drainage rules are also implemented in this model with C++. This pore-scale network is freely available in the open-source software Yade [22].

The CGAL library insures exact predicates and constructions of network. The only nontrivial operation is the computation of entry phase curvature needed to define the NW-W phase contact lines and pore throat areas to determine acting forces in Eq.9.

4 COMPARISON WITH EXPERIMENT

4.1 Numerical setup

In this section, we verify the pore-network model by comparing the simulation results with experimental data of quasi-static drainage experiment in a synthetic porous medium[6]. The medium consisted of packed glass beads, with three size classes, 0.6, 0.85 and 1.0-1.4 mm in diameter. The glass beads are contained in a column of 70 mm in length and 7 mm in diameter, with a porosity of 0.34. Drainage is carried out by pumping water out of the porous medium with a certain flow rate to maintain the system to equilibrate. A 5 mm section of the column is imaged by using X-ray micro-tomography to obtain capillary pressure-saturation ($P^c - S^w$) relationship.

In the simulation, it is unachievable to assign the pore-network (Regular Triangulation) in geometry of circular column, so we compromise by implementing model in cuboid packings. Following the experimental scene, the simulation packing is connected to the NW reservoir on the top, and to the W reservoir at the bottom.

In the research, we couldn't manage to achieve the original positioning data of glass beads in benchmark experiment[6]. But the porous medium with target PSD and porosity can be emulated by using our DEM software by the growth of spheres after randomly positioning, using the radius expansion-friction decrease (REFD) growth algorithm, a dynamic compaction method which lets one control the porosity of dense random packings [4]. So we compromise to simulate a series of repeated test on different randomly positioning packings with the consistent PSD and porosity of the experiment. In order to compare conveniently with all simulation cases, the simulation results and experiment data are both normalized to be dimensionless quantities. We represent the capillary pressure P^c by,

$$P^* = \frac{P^c \bar{D}}{\sigma^{nw}} \tag{10}$$

in which,$\bar{D}$ =0.8675 mm is the average size for PSD, $\sigma^{nw} = 7.28 \times 10^{-2} N/m$ is the W-phase (water) surface tension in contact with NW-phase (air) in 20^oC. We also assume the material of solid particles is perfectly wetting, thus the contact angle θ in simulation is 0.

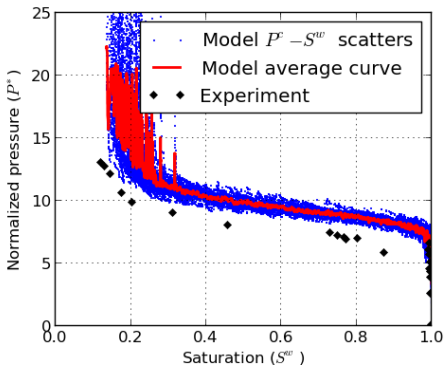

Figure 4: Comparison between simulation and experiment for primary drainage $P^c - S^w$ curves. The No. of observations of simulation is 100.

4.2 Comparison results and discussion

Using the technique described above, we compute the primary drainage process of 100 random dense packings with the same PSD and porosity. Fig.4 presents the results of these simulations, in which we gather all scattered (S^w, P^*) points of each simulation in one image. As shown in Fig.4, although all packings share the same macro-mechanics parameters, the $P^c - S^w$ curves still have a distinct variety because of micro setup, i.e., sphere positioning. Especially, the residual saturation has a great difference. We compare the average results from 100 repeating simulations with the experimental data. It shows satisfactory agreement between predicated capillary curve and obtained experimentally by Culligan et al.[6]. The unremarkable difference is mainly caused by the different specimen shapes, i.e., the simulation using cuboid column packing and experiment using circular column one. A more detailed discussion can be found in [23].

We capture one test from the series of simulation and cut a slice to observe the characteristics of invasion as shown in Fig.5. By increasing P^c, the invasion starts from the pores with larger throat, in which the entry capillary pressure is smaller (see slice-a). By comparing slices-b and c, we can find out that at certain circumstances even a slight changing in P^c can cause a notable NW-W interface movement. So such event, i.e., Haines jump, can involve a cluster of pores, causing a obvious discontinuous decrease of W-phase content. In slice-d showing the finish of test, even under a large P^c, there is no changing in saturation, which means such W-phase is entrapped by NW-phase.

5 CONCLUSIONS

A pore-scale network model of quasi-static two-phase flow in dense sphere packings has been proposed. The model can satisfactorily replicate the phenomenon of primary drainage in synthetic porous medium. The pore space is efficiently represented by means of a Regular Triangulation and the entry pore throat geometry is mathematically determined by the equilibrium of the pore system. The key methods of this model are the calculation

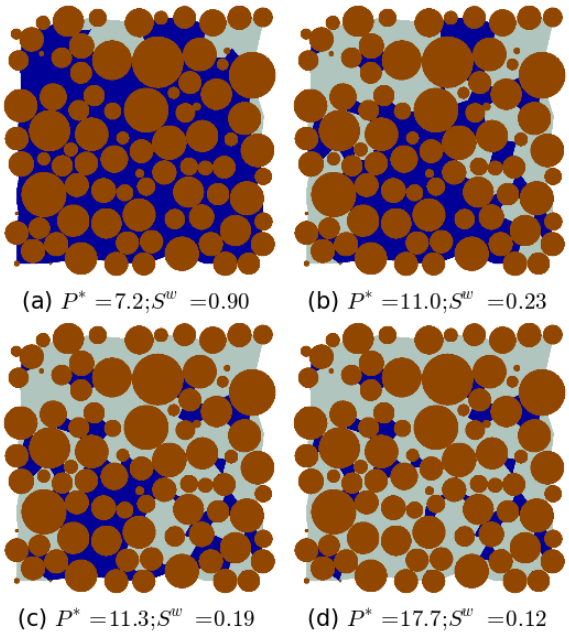

Figure 5: The process of drainage, NW-phase invade from top. Brown (gray) is solid phase, blue (black) is W-phase, and light cyan (white) is NW-phase, see color version of this figure in the HTML.

of the entry capillary pressure applied by the fluids and the prediction of the displacements of phases. Expressions of the local capillary force and tension force induced on the NW-W interface of pore throat have been derived, which are based on Young-Laplace equation and local pore geometry. The definition of entry capillary pressure is based on MS-P (Mayer-Stowe-Princen) method, which follows the balance of forces for NW-W interface in quasi-static regime. The drainage process is represented by the invasion of NW-phase when the threshold value is reached.

The key feature of the model is its capability to entrap the receding W-phase, indicating the residual saturation. A dynamic search algorithm is applied to identify whether local disconnection causes large clusters of wetting pores to get disconnected with wetting phase reservoir. For validation purpose, the model has been used for simulating primary drainage experiments carried out in a glass bead packing. The simulated curve is in agreement with experiment one, which means the capability of the pore-scale network model for simulating a real porous medium can be verified.

6 Appendix: Calculation of capillary force and tension force for a pore throat

In this appendix, we will explicitly solve the capillary force F^p and tension force T^σ acting on pore throat by using pore throat radius.

In a given pore throat (see Fig.2b), the radii and positions of neighboring solid particles are known. Let's denote a possible pore throat radius by r_c and suppose the porous media

being in perfectly wetting condition, i.e., contact angle $\theta = 0$. The contact line between NW and W phases would be tangent with solid surface.

In triangulation domain ΔABC, the area may be written as follows:

$$A_{\Delta ABC} = \frac{1}{2} bc \sin \alpha \tag{11}$$

Using laws of cosines, we can write the following equations to solve α, β and γ in ΔABC,

$$a^2 = b^2 + c^2 - 2bc \cos \alpha \tag{12}$$

$$b^2 = a^2 + c^2 - 2ac \cos \beta \tag{13}$$

$$c^2 = a^2 + b^2 - 2ab \cos \gamma \tag{14}$$

Likewise, the areas and φ_{ij} in ΔAO_3B, ΔBO_1C and ΔAO_2C can be obtained.

To solve F^p, the total area of liquid bridge A_{lb} within pore throat section can be calculated:

$$\begin{aligned} A_{lb} = &(A_{\Delta AO_3B} - 0.5R_1^2\varphi_{31} - 0.5R_2^2\varphi_{32} - 0.5r_c^2\varphi_{33}) \\ &+(A_{\Delta BO_1C} - 0.5R_2^2\varphi_{12} - 0.5R_3^2\varphi_{13} - 0.5r_c^2\varphi_{11}) \\ &+(A_{\Delta AO_2C} - 0.5R_1^2\varphi_{21} - 0.5R_3^2\varphi_{23} - 0.5r_c^2\varphi_{22}) \end{aligned} \tag{15}$$

The area of pore throat A_n may be written as:

$$A_n = A_{\Delta ABC} - A_{lb} - 0.5R_1^2\alpha - 0.5R_2^2\beta - 0.5R_3^2\gamma \tag{16}$$

Combining Eq.4, 5 and 16, the explicit expression of F^p would be obtained.

Because of the perfectly wetting assumption, T^σ acting on multi-phase contact lines in Eq.8 can be simplified by,

$$T^\sigma(r_c) = (L_{nw} + L_{ns})\sigma^{nw} \tag{17}$$

The contact lines L_{nw} and L_{ns} can be obtained as follows:

$$L_{nw} = r_c\varphi_{11} + r_c\varphi_{22} + r_c\varphi_{33} \tag{18}$$

$$L_{ns} = R_1(\alpha - \varphi_{21} - \varphi_{31}) + R_2(\beta - \varphi_{32} - \varphi_{12}) + R_3(\gamma - \varphi_{13} - \varphi_{23}) \tag{19}$$

Combining Eq.17, 18 and 19, the explicit expression of T^σ would be calculated.

REFERENCES

[1] J. Boissonnat, O. Devillers, S. Pion, M. Teillaud, and M. Yvinec. Triangulations in cgal. *Computational Geometry: Theory and Applications*, 22:5–19, 2002.

[2] S. Bryant and M. Blunt. Prediction of relative permeability in simple porous media. *Phys. Rev. A*, 46:2004–2011, Aug 1992.

[3] E. Catalano. *A pore-scale coupled hydromechanical model for biphasic granular media.* PhD thesis, Grenoble INP, 2012.

[4] B. Chareyre, L. Briançon, and P. Villard. Theoretical versus experimental modelling of the anchorage capacity of geotextiles in trenches. *Geosynthetics International*, 9(2):97–123, 2002.

[5] B. Chareyre, A. Cortis, E. Catalano, and E. Barthélemy. Pore-scale modeling of viscous flow and induced forces in dense sphere packings. *Transp. Porous Med.*, 92:473–493, 2012.

[6] K. Culligan, D. Wildenschild, B. Christensen, W. Gray, M. Rivers, and A. Tompson. Interfacial area measurements for unsaturated flow through a porous medium. *Water Resour. Res.*, 40(12), 2004.

[7] P. Cundall and O. Strack. A discrete numerical model for granular assemblies. *Geotechnique*, (29):47–65, 1979.

[8] H. Edelsbrunner and N. R. Shah. Incremental topological flipping works for regular triangulations. *Algorithmica*, 15(6):223–241, 1996.

[9] I. Fatt. The network model of porous media i, ii, iii. *Trans AIME*, 207:144–181, 1956.

[10] M. Gladkikh and S. Bryant. Prediction of interfacial areas during imbibition in simple porous media. *Advances in Water Resources*, 26(6):609 – 622, 2003.

[11] V. Joekar-Niasar, M. Prodanović, D. Wildenschild, and S. Hassanizadeh. Network model investigation of interfacial area, capillary pressure and saturation relationships in granular porous media. *Water Resour. Res.*, 46, 2010.

[12] R. Lenormand. Liquids in porous media. *Journal of Physics: Condensed Matter*, 2(S):SA79, 1990.

[13] R. Lenormand, E. Touboul, and C. Zarcone. Numerical models and experiments on immiscible displacements in porous media. *Journal of Fluid Mechanics*, 189:165–187, 1988.

[14] S. Ma, G. Mason, and N. Morrow. Effect of contact angle on drainage and imbibition in regular polygonal tubes. *Colloids and Surfaces A: Physicochemical and Engineering Aspects*, 117(3):273 – 291, 1996.

[15] G. Mason and D. Mellor. Simulation of drainage and imbibition in a random packing of equal spheres. *Journal of Colloid and Interface Science*, 176(1):214 – 225, 1995.

[16] R. Mayer and R. Stowe. Mercury porosimetrybreakthrough pressure for penetration between packed spheres. *Journal of Colloid Science*, 20(8):893 – 911, 1965.

[17] P. Øren, S. Bakke, and O. Arntzen. Extending predictive capabilities to network models. *SPE Journal*, 3(4):324–336, 1998.

[18] H. Princen. Capillary phenomena in assemblies of parallel cylinders: Ii. capillary rise in systems with more than two cylinders. *Journal of Colloid and Interface Science*, 30(3):359 – 371, 1969.

[19] R.Chandler, J.Koplik, K.Lerman, and J.F.Willemsen. Capillary displacement and percolation in porous media. *Journal of Fluid Mechanics*, 119:249–267, 6 1982.

[20] L. Scholtes, B. Chareyre, F. Nicot, and F. Darve. Micromechanics of granular materials with capillary effects. *International Journal of Engineering Science*, 47(1112):1460 – 1471, 2009.

[21] L. Scholtes, P. Hicher, F. Nicot, B. Chareyre, and F. Darve. On the capillary stress tensor in wet granular materials. *Int. J. Numer. Anal. Meth. Geomech.*, 33(10):1289–1313, 2009.

[22] V. Smilauer, E. Catalano, B. Chareyre, S. Dorofeenko, J. Duriez, A. Gladky, J. Kozicki, C. Modenese, L. Scholtes, L. Sibille, J. Stransky, and K. Thoeni. Yade Reference Documentation. In V. Smilauer, editor, *Yade Documentation*. 2010. http://yade-dem.org/doc/.

[23] C. Yuan, B. Chareyre, and F. Darve. Pore-scale simulations of drainage in granular materials: finite size effects and the representative elementary volume (submitted to journal). *Advances in Water Resources*, 2015.